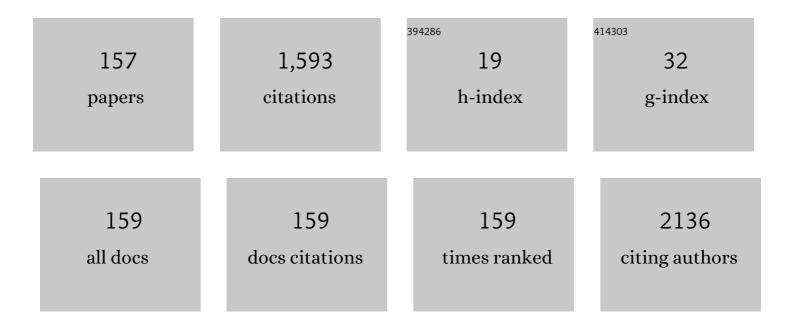
Osamu Ichii

List of Publications by Year in descending order

Source: https://exaly.com/author-pdf/5574890/publications.pdf Version: 2024-02-01



Осами Існи

#	Article	IF	CITATIONS
1	Decreased miR-26a Expression Correlates with the Progression of Podocyte Injury in Autoimmune Glomerulonephritis. PLoS ONE, 2014, 9, e110383.	1.1	107
2	Altered expression of microRNA miR-146a correlates with the development of chronic renal inflammation. Kidney International, 2012, 81, 280-292.	2.6	105
3	Podocyte Injury Caused by Indoxyl Sulfate, a Uremic Toxin and Aryl-Hydrocarbon Receptor Ligand. PLoS ONE, 2014, 9, e108448.	1.1	77
4	MicroRNAs associated with the development of kidney diseases in humans and animals. Journal of Toxicologic Pathology, 2018, 31, 23-34.	0.3	68
5	PMab-52: Specific and Sensitive Monoclonal Antibody Against Cat Podoplanin for Immunohistochemistry. Monoclonal Antibodies in Immunodiagnosis and Immunotherapy, 2017, 36, 224-230.	0.8	57
6	Local overexpression of interleukin-1 family, member 6 relates to the development of tubulointerstitial lesions. Laboratory Investigation, 2010, 90, 459-475.	1.7	47
7	A conserved region in the prM protein is a critical determinant in the assembly of flavivirus particles. Journal of General Virology, 2012, 93, 27-38.	1.3	42
8	Urinary exosome-derived microRNAs reflecting the changes of renal function and histopathology in dogs. Scientific Reports, 2017, 7, 40340.	1.6	41
9	Tick-borne flaviviruses alter membrane structure and replicate in dendrites of primary mouse neuronal cultures. Journal of General Virology, 2014, 95, 849-861.	1.3	38
10	Rapid specimen preparation to improve the throughput of electron microscopic volume imaging for three-dimensional analyses of subcellular ultrastructures with serial block-face scanning electron microscopy. Medical Molecular Morphology, 2016, 49, 154-162.	0.4	33
11	Characterization of mouse mediastinal fat-associated lymphoid clusters. Cell and Tissue Research, 2014, 357, 731-741.	1.5	28
12	Overexpression of Toll-like receptor 8 correlates with the progression of podocyte injury in murine autoimmune glomerulonephritis. Scientific Reports, 2014, 4, 7290.	1.6	28
13	Effects of a mixture of medetomidine, midazolam and butorphanol on anesthesia and blood biochemistry and the antagonizing action of atipamezole in hamsters. Journal of Veterinary Medical Science, 2017, 79, 1230-1235.	0.3	25
14	Local CD34-positive capillaries decrease in mouse models of kidney disease associating with the severity of glomerular and tubulointerstitial lesions. BMC Nephrology, 2017, 18, 280.	0.8	25
15	Potential Role of Nonneutralizing IgA Antibodies in Cross-Protective Immunity against Influenza A Viruses of Multiple Hemagglutinin Subtypes. Journal of Virology, 2020, 94, .	1.5	25
16	Modified scanning electron microscopy reveals pathological crosstalk between endothelial cells and podocytes in a murine model of membranoproliferative glomerulonephritis. Scientific Reports, 2018, 8, 10276.	1.6	23
17	Effects of PCB exposure on serum thyroid hormone levels in dogs and cats. Science of the Total Environment, 2019, 688, 1172-1183.	3.9	22
18	Altered balance of inhibitory and active Fc gamma receptors in murine autoimmune glomerulonephritis. Kidney International, 2008, 74, 339-347.	2.6	21

#	Article	IF	CITATIONS
19	MicroRNA expression profiling of cat and dog kidneys. Research in Veterinary Science, 2014, 96, 299-303.	0.9	21
20	Food Yellow4 reprotoxicity in relation to localization of DMC1 and apoptosis in rat testes: Roles of royal jelly and cod liver oil. Ecotoxicology and Environmental Safety, 2019, 169, 696-706.	2.9	21
21	Analysis of the mechanism of radiation-induced upregulation of mitochondrial abundance in mouse fibroblasts. Journal of Radiation Research, 2017, 58, 292-301.	0.8	20
22	Comparative analysis of mediastinal fatâ€associated lymphoid cluster development and lung cellular infiltration in murine autoimmune disease models and the corresponding normal control strains. Immunology, 2016, 147, 30-40.	2.0	19
23	Overexpression of toll-like receptor 9 correlates with podocyte injury in a murine model of autoimmune membranoproliferative glomerulonephritis. Autoimmunity, 2018, 51, 386-398.	1.2	19
24	IL-36α Regulates Tubulointerstitial Inflammation in the Mouse Kidney. Frontiers in Immunology, 2017, 8, 1346.	2.2	17
25	Effects of topiroxostat in hyperuricemic patients with chronic kidney disease. Clinical and Experimental Nephrology, 2018, 22, 337-345.	0.7	17
26	Histopathological Correlations between Mediastinal Fat-Associated Lymphoid Clusters and the Development of Lung Inflammation and Fibrosis following Bleomycin Administration in Mice. Frontiers in Immunology, 2018, 9, 271.	2.2	17
27	Quantitative and Qualitative Urinary Cellular Patterns Correlate with Progression of Murine Glomerulonephritis. PLoS ONE, 2011, 6, e16472.	1.1	17
28	Sex-related differences in autoimmune-induced lung lesions in MRL/MpJ-faslpr mice are mediated by the development of mediastinal fat-associated lymphoid clusters. Autoimmunity, 2017, 50, 306-316.	1.2	16
29	Newly diagnosed IgA nephropathy with gross haematuria following COVID-19 vaccination. QJM - Monthly Journal of the Association of Physicians, 2022, 115, 28-29.	0.2	16
30	Close Relations between Podocyte Injuries and Membranous Proliferative Glomerulonephritis in Autoimmune Murine Models. American Journal of Nephrology, 2013, 38, 27-38.	1.4	15
31	Thyroid-like low-grade nasopharyngeal papillary adenocarcinoma: A case report. Molecular and Clinical Oncology, 2016, 5, 693-696.	0.4	15
32	Close pathological correlations between chronic kidney disease and reproductive organ-associated abnormalities in female cotton rats. Experimental Biology and Medicine, 2018, 243, 418-427.	1.1	14
33	Cotton rat (Sigmodon hispidus) develops metabolic disorders associated with visceral adipose inflammation and fatty pancreas without obesity. Cell and Tissue Research, 2019, 375, 483-492.	1.5	14
34	MRL/MpJ- <i>Fas</i> ^{lpr} mice show abnormalities in ovarian function and morphology with the progression of autoimmune disease. Autoimmunity, 2015, 48, 402-411.	1.2	13
35	Wall thickness control in biotubes prepared using type-C mold. Journal of Artificial Organs, 2018, 21, 387-391.	0.4	13
36	Molecular Pathology of Murine Ureteritis Causing Obstructive Uropathy with Hydronephrosis. PLoS ONE, 2011, 6, e27783.	1.1	13

#	Article	IF	CITATIONS
37	Analysis of factors decreasing testis weight in MRL mice. Mammalian Genome, 2010, 21, 153-161.	1.0	12
38	Altered ciliary morphofunction in the oviductal infundibulum of systemic autoimmune disease-prone MRL/MpJ-Faslpr/lpr mice. Cell and Tissue Research, 2020, 380, 627-641.	1.5	12
39	Characterisation of a cysteine protease from poultry red mites and its potential use as a vaccine for chickens. Parasite, 2021, 28, 9.	0.8	12
40	Ovarian cysts in MRL / MpJ mice are derived from the extraovarian rete: a developmental study. Journal of Anatomy, 2011, 219, 743-755.	0.9	11
41	Female cotton rats (Sigmodon hispidus) develop chronic anemia with renal inflammation and cystic changes. Histochemistry and Cell Biology, 2016, 146, 351-362.	0.8	11
42	A case of neuronal intranuclear inclusion disease associated with lupus nephritis–like nephropathy. ENeurologicalSci, 2018, 10, 28-30.	0.5	11
43	Urinary Exosome-Derived microRNAs Reflecting the Changes in Renal Function in Cats. Frontiers in Veterinary Science, 2018, 5, 289.	0.9	11
44	An experimental study of menopause induced by bilateral ovariectomy and mechanistic effects of mesenchymal stromal cell therapy on the parotid gland of a rat model. Annals of Anatomy, 2018, 220, 9-20.	1.0	11
45	Immunohistochemical localization of renin, NO synthase-1, and cyclooxygenase-2 in rodent kidney. Histology and Histopathology, 2008, 23, 143-50.	0.5	11
46	Vasculature-Associated Lymphoid Tissue: A Unique Tertiary Lymphoid Tissue Correlates With Renal Lesions in Lupus Nephritis Mouse Model. Frontiers in Immunology, 2020, 11, 595672.	2.2	11
47	Ca ²⁺ -activated Cl ^{â^'} channel currents in mammary secretory cells from lactating mouse. American Journal of Physiology - Cell Physiology, 2016, 311, C808-C819.	2.1	10
48	Molecular characterization of three Sarcocystis spp. from wild sika deer (Cervus nippon yesoensis) in Hokkaido, Japan. Veterinary Parasitology: Regional Studies and Reports, 2019, 18, 100327.	0.3	10
49	PD-L1 expression in equine malignant melanoma and functional effects of PD-L1 blockade. PLoS ONE, 2020, 15, e0234218.	1.1	10
50	REV-ERB agonist suppresses IL-17 production in Î ³ ÎT cells and improves psoriatic dermatitis in a mouse model. Biomedicine and Pharmacotherapy, 2021, 144, 112283.	2.5	10
51	Development of mPMab-1, a Mouse–Rat Chimeric Antibody Against Mouse Podoplanin. Monoclonal Antibodies in Immunodiagnosis and Immunotherapy, 2017, 36, 77-79.	0.8	9
52	First molecular detection of Sarcocystis ovalis in the intestinal mucosa of a Japanese jungle crow (Corvus macrorhynchos) in Hokkaido, Japan. Veterinary Parasitology: Regional Studies and Reports, 2017, 10, 54-57.	0.3	9
53	Drug reaction with eosinophilia and systemic symptoms/drugâ€induced hypersensitivity syndrome (DRESS/DIHS) caused by levofloxacin in a patient with systemic scleroderma, rheumatoid arthritis, and Sjogren syndrome. Contact Dermatitis, 2019, 80, 253-254.	0.8	9
54	Species Specific Differences in the Ratio of Short to Long Loop Nephrons in the Kidneys of Laboratory Rodents. Experimental Animals, 2006, 55, 473-476.	0.7	8

#	Article	IF	CITATIONS
55	Rodent Renal Structure Differs among Species. Journal of Veterinary Medical Science, 2006, 68, 439-445.	0.3	8
56	A case of acute kidney injury caused by granulomatous interstitial nephritis associated with sarcoidosis. CEN Case Reports, 2018, 7, 34-38.	0.5	8
57	Immune-associated renal disease found in caspase 3-deficient mice. Cell and Tissue Research, 2020, 379, 323-335.	1.5	8
58	Spatiotemporal histological changes observed in mouse subcutaneous tissues during the foreign body reaction to silicone. Journal of Biomedical Materials Research - Part A, 2021, 109, 1220-1231.	2.1	8
59	Cotton rats (Sigmodon hispidus) possess pharyngeal pouch remnants originating from different primordia. Histology and Histopathology, 2018, 33, 555-565.	0.5	8
60	Hydrogen sulfide activates TRPA1 and releases 5-HT from epithelioid cells of the chicken thoracic aorta. Comparative Biochemistry and Physiology Part - C: Toxicology and Pharmacology, 2016, 187, 43-49.	1.3	7
61	In vitro characterization of adipocyte plasma membrane-associated protein from poultry red mites, Dermanyssus gallinae, as a vaccine antigen for chickens. Vaccine, 2021, 39, 6057-6066.	1.7	7
62	Sulfated glycans containing NeuAcα2-3Gal facilitate the propagation of human H1N1 influenza A viruses in eggs. Virology, 2021, 562, 29-39.	1.1	7
63	Close Association between Altered Urine–Urothelium Barrier and Tertiary Lymphoid Structure Formation in the Renal Pelvis during Nephritis. Journal of the American Society of Nephrology: JASN, 2022, 33, 88-107.	3.0	7
64	Quantitative trait locus analysis of ovarian cysts derived from rete ovarii in MRL/MpJ mice. Mammalian Genome, 2010, 21, 162-171.	1.0	6
65	The Onset of Heat-Induced Testicular Calcification in Mice. American Journal of Pathology, 2014, 184, 2480-2492.	1.9	6
66	Slc:Wistar/ST rats develop unilateral thyroid dysgenesis: A novel animal model of thyroid hemiagenesis. PLoS ONE, 2019, 14, e0221939.	1.1	6
67	Histopathological features of the proper gastric glands in FVB/N-background mice carrying constitutively-active aryl-hydrocarbon receptor. BMC Gastroenterology, 2019, 19, 102.	0.8	6
68	A Rare Presentation of Hypermagnesemia Associated with Acute Kidney Injury due to Hypercalcemia. Internal Medicine, 2019, 58, 1123-1126.	0.3	6
69	Age-related glomerular lesions with albuminuria in male cotton rats. Histochemistry and Cell Biology, 2020, 153, 27-36.	0.8	6
70	Developmental Changes of the Ovary in Neonatal Cotton Rat (Sigmodon hispidus). Frontiers in Physiology, 2020, 11, 601927.	1.3	6
71	Compartmentalization of interleukin 36 subfamily according to inducible and constitutive expression in the kidneys of a murine autoimmune nephritis model. Cell and Tissue Research, 2021, 386, 59-77.	1.5	6
72	Characterization of a copper transporter 1 from <i>Dermanyssus gallinae</i> as a vaccine antigen. Parasitology, 2022, 149, 105-115.	0.7	6

Озами Існіі

#	Article	IF	CITATIONS
73	Abnormal Blood Coagulation and Kidney Damage in Aged Hamsters Infected with Severe Acute Respiratory Syndrome Coronavirus 2. Viruses, 2021, 13, 2137.	1.5	6
74	In vitro evaluation of a cysteine protease from poultry red mites, Demanyssus gallinae, as a vaccine antigen for chickens. Poultry Science, 2022, 101, 101638.	1.5	6
75	Turkeys possess diverse Sial±2-3Cal glycans that facilitate their dual susceptibility to avian influenza viruses isolated from ducks and chickens. Virus Research, 2022, 315, 198771.	1.1	6
76	MRL/MpJ mice show unique pathological features after experimental kidney injury. Histology and Histopathology, 2016, 31, 189-204.	0.5	6
77	Degenerative and regenerative features of myofibers differ among skeletal muscles in a murine model of muscular dystrophy. Journal of Muscle Research and Cell Motility, 2016, 37, 153-164.	0.9	5
78	Comparative Analyses of the Antiviral Activities of IgG and IgA Antibodies to Influenza A Virus M2 Protein. Viruses, 2020, 12, 780.	1.5	5
79	Pathological Alternations of Mediastinal Fat-Associated Lymphoid Cluster and Lung in a Streptozotocin-Induced Diabetic Mouse Model. Microscopy and Microanalysis, 2021, 27, 187-200.	0.2	5
80	Genomic analysis of the appearance of testicular oocytes in MRL/MpJ mice. Mammalian Genome, 2012, 23, 741-748.	1.0	4
81	Relationship between Numerous Mast Cells and Early Follicular Development in Neonatal MRL/MpJ Mouse Ovaries. PLoS ONE, 2013, 8, e77246.	1.1	4
82	Decrease in an Inwardly Rectifying Potassium Conductance in Mouse Mammary Secretory Cells after Forced Weaning. PLoS ONE, 2015, 10, e0141131.	1.1	4
83	Spatiotemporal distribution of extracellular matrix changes during mouse duodenojejunal flexure formation. Cell and Tissue Research, 2016, 365, 367-379.	1.5	4
84	Tissue distribution and characterization of feline cytochrome P450 genes related to polychlorinated biphenyl exposure. Comparative Biochemistry and Physiology Part - C: Toxicology and Pharmacology, 2019, 226, 108613.	1.3	4
85	Altered morpho-functional features of bones in autoimmune disease-prone BXSB/MpJ- <i>Yaa</i> mice. Experimental Biology and Medicine, 2019, 244, 333-343.	1.1	4
86	Morphological and molecular identification of cyathostomine gastrointestinal nematodes of Murshidia and Quilonia species from Asian elephants in Myanmar. International Journal for Parasitology: Parasites and Wildlife, 2020, 11, 294-301.	0.6	4
87	BXSB/MpJ-Yaa mouse model of systemic autoimmune disease shows increased apoptotic germ cells in stage XII of the seminiferous epithelial cycle. Cell and Tissue Research, 2020, 381, 203-216.	1.5	4
88	Anatomy and histology of the foramen of ovarian bursa opening to the peritoneal cavity and its changes in autoimmune diseaseâ€prone mice. Journal of Anatomy, 2021, 238, 73-85.	0.9	4
89	Unique morphological characteristics in the ovary of cotton rat (<i>Sigmodon) Tj ETQq1 1 0.784314 rgBT</i>	Overlock	10
90	Characterization of a Novel Cysteine Protease Inhibitor from Poultry Red Mites: Potential Vaccine for	2.1	4

Chickens. Vaccines, 2021, 9, 1472.

2.1

#	Article	IF	CITATIONS
91	Genital organ-associated lymphoid tissues arranged in a ring in the mucosa of cow vaginal vestibules. Research in Veterinary Science, 2022, 145, 147-158.	0.9	4
92	Genomic Analysis of the Appearance of Ovarian Mast Cells in Neonatal MRL/MpJ Mice. PLoS ONE, 2014, 9, e100617.	1.1	3
93	Low expression of cyclooxygenase-2 in chronic kidney disease in young dogs. Research in Veterinary Science, 2016, 109, 71-73.	0.9	3
94	Pulmonary hypertension due to unclassified interstitial lung disease in a Pembroke Welsh corgi. Journal of Veterinary Medical Science, 2018, 80, 939-944.	0.3	3
95	Restricted localization of ultimobranchial body remnants and parafollicular cells in the one-humped camel (<i>Camelus dromedarius</i>). Journal of Veterinary Medical Science, 2018, 80, 1368-1372.	0.3	3
96	Unique histological features of the tail skin of cotton rat (Sigmodon hispidus) related to caudal autotomy. Biology Open, 2021, 10, .	0.6	3
97	Possible Crosstalk of the Immune Cells within the Lung and Mediastinal Fat-Associated Lymphoid Clusters in the Acute Inflammatory Lung Asthma-Like Mouse Model. International Journal of Molecular Sciences, 2021, 22, 6878.	1.8	3
98	Podocyte Injury Through Interaction Between Tlr8 and Its Endogenous Ligand miR-21 in Obstructed and Its Collateral Kidney. Frontiers in Immunology, 2020, 11, 606488.	2.2	3
99	Histopathological changes in tear-secreting tissues and cornea in a mouse model of autoimmune disease. Experimental Biology and Medicine, 2020, 245, 999-1008.	1.1	3
100	Autoimmune polyglandular syndrome type 3 variant in rheumatoid arthritis. Romanian Journal of Internal Medicine = Revue Roumaine De Medecine Interne, 2020, 58, 40-43.	0.3	3
101	Membranous Nephropathy Associated With Multicentric Castleman Disease—Efficacy of Interleukin 6 Antibody for Nephrotic Syndrome. Journal of Clinical Rheumatology, 2022, 28, e1-e2.	0.5	3
102	Clarifying expression patterns by renal lesion using transcriptome analysis and vanin-1 as a potential novel biomarker for renal injury in chickens. Poultry Science, 2022, 101, 102011.	1.5	3
103	Renal thrombotic microangiopathy caused by bevacizumab. Nephrology, 2018, 23, 378-379.	0.7	2
104	Bilateral striopallidodentate calcinosis associated with Sjögren's syndrome and IgDλ monoclonal gammopathy of undetermined significance. Joint Bone Spine, 2018, 85, 243-245.	0.8	2
105	Macrophage activation syndrome associated with systemic lupus erythematosus treated successfully with the combination of steroid pulse, immunoglobulin and tacrolimus. Romanian Journal of Internal Medicine = Revue Roumaine De Medecine Interne, 2018, 56, 117-121.	0.3	2
106	MRL/MpJ mice produce more oocytes and exhibit impaired fertilisation and accelerated luteinisation after superovulation treatment. Reproduction, Fertility and Development, 2019, 31, 760.	0.1	2
107	The intratumor heterogeneity of <i>TP53</i> gene mutations in canine histiocytic sarcoma. Journal of Veterinary Medical Science, 2019, 81, 353-356.	0.3	2
108	Is recurrent Kikuchi-Fujimoto disease a precursor to systemic lupus erythematosus?. Romanian Journal of Internal Medicine = Revue Roumaine De Medecine Interne, 2019, 57, 72-77.	0.3	2

#	Article	IF	CITATIONS
109	Takayasu Arteritis Presenting as Renovascular Hypertension. Journal of Clinical Rheumatology, 2020, 26, e94-e94.	0.5	2
110	Reactive Arthritis Caused by Rothia mucilaginosa in an Elderly Diabetic Patient. Journal of Clinical Rheumatology, 2020, 26, e303-e304.	0.5	2
111	Unique Running Pattern and Mucosal Morphology Found in the Colon of Cotton Rats. Frontiers in Physiology, 2020, 11, 587214.	1.3	2
112	Nonsteroidal Anti-Inflammatory Drug-Induced Small Bowel Stricture in Rheumatoid Arthritis. Journal of Clinical Rheumatology, 2021, 27, e86-e87.	0.5	2
113	Castrated autoimmune glomerulonephritis mouse model shows attenuated glomerular sclerosis with altered parietal epithelial cell phenotype. Experimental Biology and Medicine, 2021, 246, 1318-1329.	1.1	2
114	Immunotactoid glomerulopathy associated with monoclonal gammopathy. Lancet, The, 2021, 397, 2081.	6.3	2
115	Novel polychrome staining distinguishing osteochondral tissue and bone cells in decalcified paraffin sections. Cell and Tissue Research, 2021, 385, 727-737.	1.5	2
116	A Case of Behçet Disease Concurrent With Giant Saccular Abdominal Aortic Aneurysm. Journal of Clinical Rheumatology, 2021, 27, e107-e108.	0.5	2
117	Anti-Ku Antibody-Related Scleroderma-Polymyositis Overlap Syndrome Associated With Hypothyroid Myopathy. Journal of Clinical Rheumatology, 2021, 27, e200-e201.	0.5	2
118	The Ameliorative Effect of Dexamethasone on the Development of Autoimmune Lung Injury and Mediastinal Fat-Associated Lymphoid Clusters in an Autoimmune Disease Mouse Model. International Journal of Molecular Sciences, 2022, 23, 4449.	1.8	2
119	Modified foreign body reaction to silicone imbedded in subcutaneous tissues by different mouse systemic immune conditions. Journal of Biomedical Materials Research - Part A, 2022, 110, 1921-1931.	2.1	2
120	Testicular oocytes in MRL/MpJ mice possess similar morphological, genetic, and functional characteristics to ovarian oocytes. Mechanisms of Development, 2015, 137, 23-32.	1.7	1
121	Hydronephrosis with ureteritis developed in C57BL/6N mice carrying the congenic region derived from MRL/MpJ-type chromosome 11. Autoimmunity, 2017, 50, 114-124.	1.2	1
122	Ovarian mast cells migrate toward ovary-fimbria connection in neonatal MRL/MpJ mice. PLoS ONE, 2018, 13, e0196364.	1.1	1
123	Abnormal Morphology of Distal Tubular Epithelial Cells Is Regulated by Genetic Factors Derived from Mouse Chromosome 12. American Journal of Pathology, 2018, 188, 2120-2138.	1.9	1
124	Analysis for genetic loci controlling protoscolex development in the Echinococcus multilocularis infection using congenic mice. Infection, Genetics and Evolution, 2018, 65, 65-71.	1.0	1
125	Slc:Hartley guinea pigs frequently possess duplication of the caudal vena cava. Experimental Animals, 2019, 68, 465-470.	0.7	1
126	Overlapping Syndrome of Systemic Scleroderma and Cryoglobulinemic Vasculitis. American Journal of Medicine, 2019, 132, e589-e590.	0.6	1

#	Article	IF	CITATIONS
127	IgA-Proliferative Glomerulonephritis with Monoclonal Immunoglobulin Deposits. American Journal of Medicine, 2019, 132, e542-e545.	0.6	1
128	Hepatitis C Virus-Associated Cryoglobulinemic Vasculitis. American Journal of Medicine, 2020, 133, e367-e368.	0.6	1
129	Hydroxychloroquine-Associated Hyperpigmentation in Chilblain Lupus Erythematosus. Journal of Clinical Rheumatology, 2020, 26, e192-e192.	0.5	1
130	Suppurative Osteomyelitis Incorrectly Diagnosed as Rheumatoid Arthritis. Journal of Clinical Rheumatology, 2020, 26, e261-e263.	0.5	1
131	Long-term Imaging Findings on Serial FDG PET/CT Scans in a Patient With Polymyositis. Journal of Clinical Rheumatology, 2020, 26, e174-e175.	0.5	1
132	Distal Phalanx Osteolysis and Subcutaneous Calcinosis in CREST Syndrome. Journal of Clinical Rheumatology, 2021, 27, e22-e22.	0.5	1
133	Altered Renal Pathology in an Autoimmune Disease Mouse Model After Induction of Diabetes Mellitus. Microscopy and Microanalysis, 2021, 27, 897-909.	0.2	1
134	Comparison of Ovarian Morphology and Follicular Disturbances between Two Inbred Strains of Cotton Rats (Sigmodon hispidus). Animals, 2021, 11, 1768.	1.0	1
135	Dual Effect of Bleomycin on Histopathological Features of Lungs and Mediastinal Fat-Associated Lymphoid Clusters in an Autoimmune Disease Mouse Model. Frontiers in Immunology, 2021, 12, 665100.	2.2	1
136	Crescentic glomerulonephritis induced by antiâ€vascular endothelial growth factor receptor 2 antibody. Nephrology, 2021, , .	0.7	1
137	Altered hepatic cytochrome P450 expression in cats after chronic exposure to decabromodiphenyl ether (BDE-209). Journal of Veterinary Medical Science, 2020, 82, 978-982.	0.3	1
138	Jaccoudâ \in Ms arthropathy in the elderly. Rheumatology, 2021, , .	0.9	1
139	Morphofunctional analysis of antigen uptake mechanisms following sublingual immunotherapy with beads in mice. PLoS ONE, 2018, 13, e0201330.	1.1	0
140	Tissue-specific variation in 5Ê ¹ -terminal exons of mouse Anoctamin 1 transcript induces N-terminal variation of its protein via alternative translational start sites. Biochemical and Biophysical Research Communications, 2018, 503, 1710-1715.	1.0	0
141	Cotton Wool Sign in Paget Disease of Bone. Internal Medicine, 2019, 58, 1809-1810.	0.3	0
142	KA-1 Application of modified SEM techniques to evaluate renal pathology. Microscopy (Oxford,) Tj ETQq0 0 0 rg	BT /Oyerlo	ock 10 Tf 50 1

143	Whole immunofluorescence staining of podocytes in fabry disease. Nephrology, 2019, 24, 135-135.	0.7	0
144	Anomalous Inferior Vena Cava in a Patient With Limited Cutaneous Systemic Sclerosis and Primary Biliary Cholangitis. Journal of Clinical Rheumatology, 2020, 26, e203-e203.	0.5	0

#	Article	IF	CITATIONS
145	Antineutrophil Cytoplasmic Antibody-Associated Hypertrophic Pachymeningitis Mimicking Petroclival Meningioma. Journal of Clinical Rheumatology, 2020, 26, e153-e154.	0.5	Ο
146	Antineutrophil cytoplasmic antibody-associated vasculitis in diffuse large B cell lymphoma. Nefrologia, 2021, 41, 215-216.	0.2	0
147	Antineutrophil cytoplasmic antibody-associated vasculitis in diffuse large B cell lymphoma. Nefrologia, 2021, 41, 215-216.	0.2	0
148	Lupus-related protein-losing enteropathy associated with pseudo–pseudo Meigs' syndrome and successfully treated with hydroxychloroquine. Romanian Journal of Internal Medicine = Revue Roumaine De Medecine Interne, 2021, .	0.3	0
149	Morphological Features of the Testis among Autoimmune Mouse Model and Healthy Strains. Microscopy and Microanalysis, 2021, 27, 1209-1217.	0.2	0
150	Haematologic malignancy-associated mucocutaneous paraneoplastic syndrome. Rheumatology, 2021, , .	0.9	0
151	Value of 18F-Fluorodeoxyglucose Positron Emission Tomography/Computed Tomography in the Diagnosis of Spondyloarthropathy-Related Aortitis. Journal of Clinical Rheumatology, 2021, 27, e116-e117.	0.5	0
152	Anti-cyclic citrullinated peptide antibody-positive rheumatoid arthritis caused by bacterial organizing pneumonia in a patient with Sjogren syndrome. Romanian Journal of Internal Medicine = Revue Roumaine De Medecine Interne, 2022, .	0.3	0
153	Primary Superior Lumbar Hernia with Nephrotic-range Orthostatic Proteinuria. Internal Medicine, 2022, , .	0.3	0
154	Immunohistochemical Expression of TGF- \hat{I}^21 in Kidneys of Cats with Chronic Kidney Disease. Veterinary Sciences, 2022, 9, 114.	0.6	0
155	Cotton rats (<i>Sigmodon hispidus</i>) with a high prevalence of hydrocephalus without clinical symptoms. Neuropathology, 2022, 42, 16-27.	0.7	0
156	Scanning electron microscopy of <i>Quilonia renniei</i> from Asian elephants revealing variation in coronal leaflet number. Parasitology, 2022, 149, 529-533.	0.7	0
157	Histopathological Impact of Bleomycin on Lung Injury and Development of Mediastinal Fat-Associated Lymphoid Clusters in the Lymphoproliferative Mouse Model. Microscopy and Microanalysis, 0, , 1-15.	0.2	Ο